ELSEVIER

Spectrochimica Acta Part A 57 (2001) 1427–1441

SPECTROCHIMICA
ACTA
PART A

www.elsevier.nl/locate/saa

Studies on unimolecular and bimolecular photoprocesses of a newly synthesized selenium compound, 7-chloro-2-phenyl-9*H*-[1]-benzopyrano[3,2-*b*]-selenophene-9-one (SeP)

A.K. De [a], S.K. De [b], A.K. Mallik [b], T. Ganguly [a,*]

[a] *Department of Spectroscopy, Indian Association for the Cultivation of Science, Jadavpur, Calcutta 700 032, India*
[b] *Department of Chemistry, Jadavpur University, Jadavpur, Calcutta 700 032, India*

Received 13 October 2000; accepted 24 October 2000

Abstract

Using steady state/time resolved spectroscopic and electrochemical techniques the spectroscopic and photophysical studies were made on a novel synthesized selenophene compound SeP in nonpolar methylcyclohexane (MCH), polar aprotic acetonitrile (ACN) and polar protic ethanol (EtOH) solvents at the ambient temperature as well as at 77 K. Both from the studies on unimolecular and bimolecular photoprocesses this selenophene compound was found to possess several electronic levels, ^1B_b, ^1L_a, ^1L_b (all are of $\pi\pi^*$ nature and ^1L_b is hidden within ^1L_a band envelop like the characteristics of most of the acenes) and $^1(n_O\pi^*)$ state arising due to carbonyl oxygen atom. In polar ACN environment this $n_O\pi^*$ state disappears because it moves within the envelop of intense ^1L_a band due to large destabilization. Large overlapping of different band systems within the ^1L_a band of SeP was confirmed from the observed depolarization effect. The lack of phosphorescence of SeP both in MCH and EtOH rigid glassy matrix at 77 K has been inferred due to large vibronic interactions between closely lying triplets of the corresponding $^1n_O\pi^*$ and ^1L_b states. From the bimolecular investigations, it reveals that SeP acts as a good electron donor in presence of the well known electron acceptor 9 cyanoanthracene (9CNA). Transient absorption spectra measured by laser flash photolysis technique demonstrate the formation of ion-pair when the acceptor is excited. From the analysis of the fluorescence quenching data it seemingly indicates that the major contribution in the diminution of the fluorescence intensity of the acceptor 9CNA in presence of SeP is not only due to the photoinduced electron transfer (ET) but also originates from static type (instantaneous) quenching processes along with external heavy atom effect. The possibility of occurrence of photoinduced ET reaction in Marcus inverted region is hinted. © 2001 Elsevier Science B.V. All rights reserved.

Keywords: Selenophene; Time resolved spectroscopy; Photoinduced electron transfer; Static quenching; Dynamic quenching

---

* Corresponding author. Tel.: +91-033-4734971/+91-33-4733073 (ext. 266); fax: +91-33-473 2805.
E-mail address: sptg@mahendra.iacs.res.in (T. Ganguly).

PII: S1386-1425(00)00487-X

1. Introduction

As the origin of life itself must have seen photophysical and photochemical acts, it appears that photophysical studies on the systems containing Se should be useful since it possesses a significant role in protecting our lives [1]. In the present investigation a novel synthesized biologically active selenium compound, 7-chloro-2-phenyl-9*H*-[1]benzopyrano[3,2-*b*]-selenophene-9-ones (SeP), was chosen, to study both of its unimolecular and bimolecular photophysical properties by steady state and time resolved spectroscopic techniques.

In bimolecular photoprocesses special attention was given to reveal the mechanism of the photoinduced electron transfer (ET) reaction, if any as studies on photoinduced ET reactions using selenium compound as one of the reacting partners are rather scarce.

The investigations were carried out both at the ambient temperature and at 77 K using steady state/time resolved spectroscopic and electrochemical techniques in nonpolar MCH as well as in polar ACN and EtOH media. The results obtained from the studies are described below.

2. Experimental

2.1. Materials and their purifications

The samples 9CNA supplied by Aldrich and SeP, which is newly synthesized (for method of synthesis and characterization, vide infra) were purified by vacuum sublimation. The solvents acetonitrile (ACN), methylcyclohexane (MCH) and ethanol (EtOH) supplied by E Marck of spectroscopic grade were distilled under reduced pressure and tested for absence of any emission in the wavelength region studied.

2.2. Experimental apparatus

The steady state electronic absorption and emission spectra of moderate to dilute (10^{-3}–10^{-6} M) solutions of the samples at ambient temperature were recorded by Shimadzu UV-VIS spectrophotometer of model 2101PC and Hitachi F-4500 Fluorescence spectrophotometer respectively. The degree of polarization (P) values were measured with UV-VIS polarizer accessories purchased from Oriel Instruments, USA by using the formula:

$$P = [I_{\mathrm{EE}} - (I_{\mathrm{BE}}/I_{\mathrm{BB}})I_{\mathrm{EB}}]/\{I_{\mathrm{EE}} + (I_{\mathrm{BE}}/I_{\mathrm{BB}})I_{\mathrm{EB}}].$$

Where I_{EE} and I_{EB} are the intensities of parallel and perpendicular polarized emission with vertically polarized excitation and I_{BB} and I_{BE} are the intensities of horizontally and vertically polarized emission when excited with horizontally polarized light. $I_{\mathrm{BE}}/I_{\mathrm{BB}}$ defines the instrumental correction factor G (polarization characteristic of the photometric system). This correction is done for any change in the sensitivity of the emission channel for the vertically and horizontally polarized components.

The fluorescence lifetimes of the samples were measured by using a time correlated single photon counting (TCSPC) fluorimeter model 199 Edinburgh Instruments U.K. having conventional L format arrangement. The excitation source consists of an all metal coaxial N_2 flash lamp with an instrumental response function of about 1.2 ns FWHM at 30 kHz repetition rate. The fluorescence decays were analyzed by using deconvolution fit over the entire decay including the rising edge. The goodness of the fit has been assessed with the help of some statistical parameters, e.g. χ^2 and Durbin–Watson (DW) values. All the solutions used for the room temperature measurements were deoxygenated by purging nitrogen gas stream for about 30 min. Electrochemical measurements were done by using PAR model 370-4 electrochemistry system incorporating a model 174A polarographic analyzer, model 175 universal programmer model RE0074X-Y recorder. Three electrode systems including SCE were used in the measurements. Tetraethylammonium perchlorate (TEAP) in ACN was used as supporting electrolyte. The value of fluorescence quantum yield (ϕ_{f}^{0}) of donor SeP in ACN fluid solution was determined at room temperature (296 K) relative to that of carbazole in the same solvent ($\phi_{\mathrm{F}}^{0} = 0.40 \pm 0.03$) [2]. Transient absorption spectra at the different delay times between the exciting and analyzing pulses were measured with the help of nanosecond flash photolysis setup (Applied Photophysics) comprises of Nd:YAG laser (DCR-11, Spectra Physics). The sample was excited by 355 nm laser light (third harmonic) (FWHM ~ 8 ns). The pulsed Xe lamp of 250 W was used as probe. The photomultiplier (IP 28) output was fed into a storage oscilloscope (TDS-540 Tektronix, 500 MHz, 1 Giga sampling, GS, s^{-1}) and the storage data were transferred to a computer through a GPIB/IEEE interface.

2.2.1. Synthesis and characterization of SeP

Among the methods reported for conversion of 2′-hydroxy-ω-cinnamylidene-acetophenones (**1** in Fig. 1) to 2-styrylchromones (**2** in Fig. 1), the selenium dioxide oxidation appears to be the oldest [3]. This reaction was originally well-known for conversion of 2′-hydroxychalcones to flavones [4]. In connection with some other problem, we required **2** and therefore carried out selenium dioxide oxidation of **1**. Thus, when **1a** (1 mmol; Fig. 1) was refluxed with selenium dioxide (1.2 mmol) in isoamyl alcohol, the starting material disappeared completly within 15 h. Chromatography of the crude product mixture over silica gel afforded **2a** (yield 52%; Fig. 1) along with an unusual product characterized as 2-phenyl-9*H*-[1]benzopyrano[3,2-*b*]selenophene-9-one (**3a**; 31%; Fig. 1) from its special features. Similarly, **3b** was obtained (35%) from **1b**. The compounds **3a** and **3b** belong to a class of heterocycles not known previously. The present photophysical investigation was done with the compound **3b** (SeP).

2.3. Analytical and spectral data of 3a and 3b

3a: m.p. 183–184°C, Anal.: Found: C, 62.69; H, 3.05%; Calcd. For $C_{17}H_{10}O_2Se$: C, 62.78; H, 3.08%. IR (Nujol, ν, cm^{-1}): 1660 (CO). ^1H NMR (300 MHz, $CDCl_3$): δ7.41–7.57 (5H, m, Ar-H), 7.62–7.73 (4H, m, Ar-H) and 8.32 (1H, dd, $J = 8$ and 1.4 Hz, H-8). ^{13}C NMR (75 MHz, $CDCl_3$): δ116.61 (C-3), 117.78 (C-5), 121.72 (C-8a), 124.70 (C-7), 125.95 (C-8), 126.42 (C-3′,5′), 129.24 (C-2′,6′), 129.90 (C-4′), 133.58 (C-6), 134.81 (C-1′), 156.14 (C-4a), 157.58 (C-2), 160.53 (C-3a), 173.14 (C-9a) and 185.90 (C-9). EIMS: m/z (rel. int.) 326(100) and 324(58.1) (M^+), 298(25.9) and 296(13.1) (M^+-CO), 218(50.1, M^+-CO-Se).

3b: m.p. 219–220°C. Anal: Found: C, 56.48; H, 2.61%; Calcd for $C_{17}H_9O_2SeCl$: C, 56.77; H, 2.52%. IR (Nujol, ν, cm^{-1}): 1660 (CO). ^1H NMR (300 MHz, $CDCl_3$): δ7.45–7.50 (4H, m, Ar-H), 7.62–7.66 (4H, m, Ar-H) and 8.28 (1H, d, $J = 2$ Hz, H-8).

According to the revised mechanism of selenium dioxide oxidation of ketones [5], their α-position becomes bonded to selenium directly, but not through oxygen [6]. Thus, the plausible mechanism delineated in Scheme 1 may be suggested the formation of **3**. That **3** was not formed by interaction of **2** with either selenium or selenium dioxide under the reaction condition employed was ascertained from negative results obtained from separate experiments involving **2** and these two reagents.

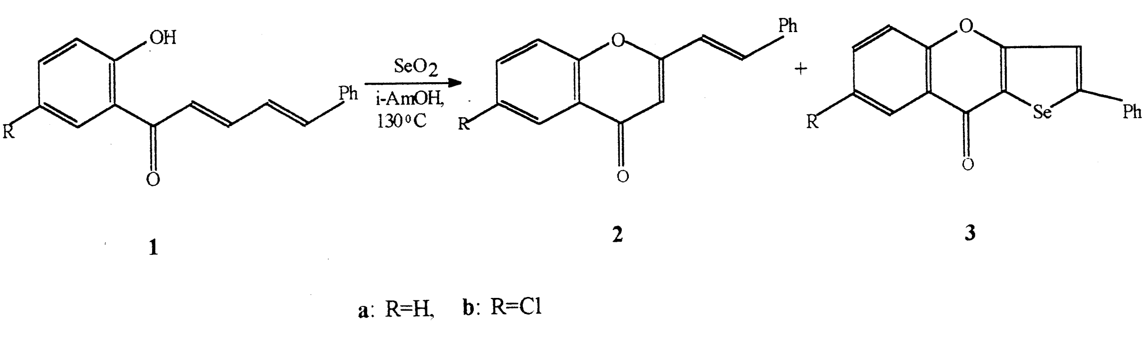

a: R=H, **b**: R=Cl

Fig. 1. Synthesis of SeP.

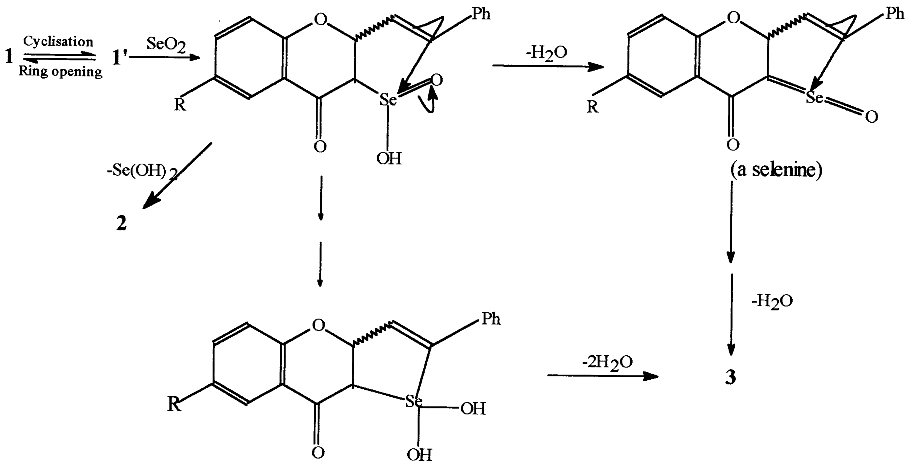

Scheme 1. Plausible mechanism of formation of SeP.

3. Results and discussion

3.1. Electronic absorption spectra of SeP in nonpolar MCH and highly polar ACN at the ambient temperature

3.1.1. Assignment of the different band systems observed in different environments

Fig. 2a reproduces the electronic absorption spectra of SeP in both MCH and ACN solvents. On comparing these spectra with those of the analogous molecule thiophenanthrene [7], which is known to possess very similar electronic spectra as anthracene, it seems logical to assign the π-electronic absorption bands of SeP at 330 nm to ^1L_a and band systems within 225–275 nm region (two peaks around 230 and 260 nm) as ^1B_b. For this molecule no ^1L_b band is apparent but it is possible, as it is the characteristics of most of the acenes, that this band might be submerged under the intense band of ^1L_a. Another important observation is that a very weak but genuine long wavelength band of broad nature was noticed for this synthesized selenium compound SeP only in nonpolar MCH environment at the wavelength region between 400 to 500 nm. The inset of Fig. 2a shows the magnified spectrum near 450 nm region showing the peak position at around 487 nm of this long wavelength absorption band. This band might be designated as singlet $n_O\pi^*$ state arising due to transition involved within the n-electron on the oxygen atom of carbonyl group (the subscript 'O' for the oxygen atom) and the antibonding π-orbital of the benzene ring. No such long wavelength band system was found in highly polar ACN solvent. Possibly due to large destabilization in this high dielectric medium this $n_O\pi^*$ band being largely blue shifted is hidden well-within the envelop of ^1L_a band system.

From Fig. 2a it is also apparent that the ^1L_a band of SeP suffers a red shift with increase of polarity of the surrounding medium, i.e. from nonpolar MCH to highly polar ACN solvent. This indicates the charge transfer character of this band which tends to stabilize in ACN.

3.2. Unimolecular photoprocesses of SeP in different solvents at the ambient temperature

3.2.1. Fluorescence of SeP in different solvents at the ambient temperature

Using the excitation wavelength at 330 nm, which is the peak position of the ^1L_a absorption band, a very weak fluorescence emission band of low quantum yield ($\phi_f = 1.32 \times 10^{-3}$) was observed for SeP in ACN surrounding medium (Fig. 2b). However, in nonpolar medium MCH, SeP becomes totally nonemissive.

From the electronic absorption spectra of SeP (Fig. 2a) it is apparent that as in MCH $^1(n_O\pi^*)$

state is the lowest excited state, the fluorescence emission should occur from this state. But possibly due to the space forbidden character of the transition involving $^1(n_O\pi^*)$ and the ground state,

SeP is nonfluorescent in MCH (Fig. 2b). On the other hand in polar solvent ACN it is possible that the change in the order of the energy levels might occur within $^1L_b(\pi\pi^*)$ and $^1(n_O\pi^*)$ states

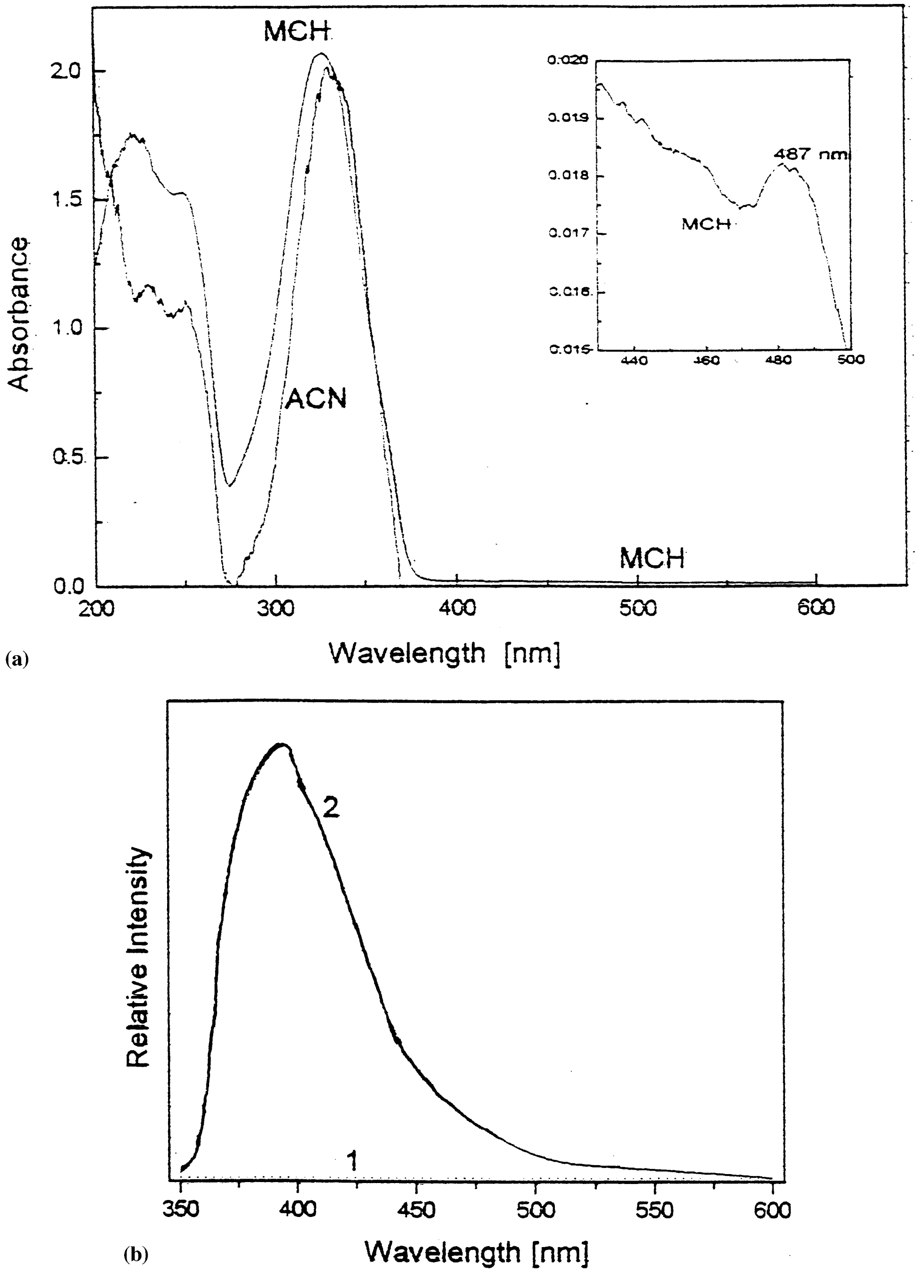

Fig. 2. (a) The electronic absorption spectra of SeP ($\sim 10^{-5}$ mol dm^{-3}) in MCH and ACN media (inset shows the magnified version of the longer wavelength band at 487 nm region in MCH) at the ambient temperature. (b) Fluorescence emission spectra of SeP ($\lambda_{ex} \sim 334$ nm; $\sim 10^{-5}$ mol dm^{-3}) in MCH (1) and in ACN solvent (2) at the ambient temperature.

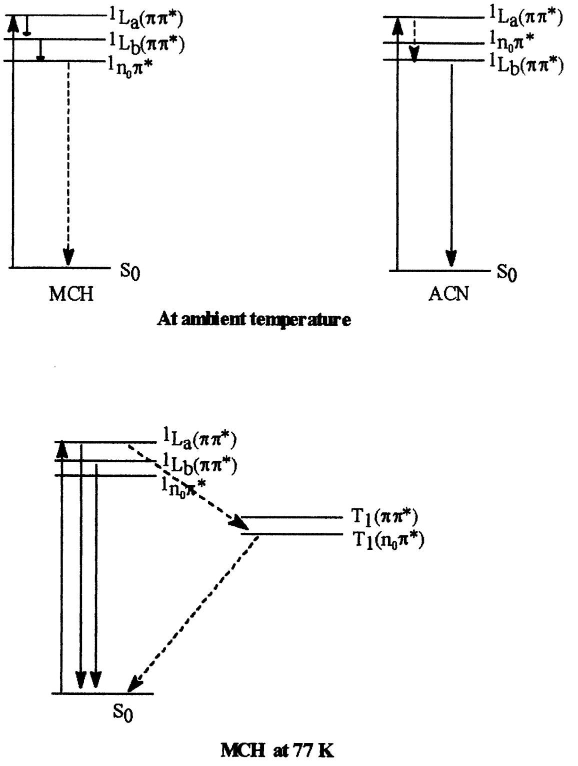

Fig. 3. Possible radiative and nonradiative deactivation scheme of photoexcited SeP in different environments.

causing the former level as the lowest emitting state. In such a situation the fluorescence emission could be expected which was actually observed in the present investigation. Very weak fluorescence intensity in ACN might be due to internal heavy atom effect as SeP contains selenium. The possible radiative and nonradiative transitions within the different electronic levels of SeP in both MCH and ACN solvents at the ambient temperature and in MCH rigid glassy matrix at 77 K (discussion on low temperature results are made below) are shown in the Fig. 3.

In order to check whether internal heavy atom effect is really responsible for weak fluorescence intensity of SeP in ACN, an attempt was made to measure low temperature (77 K) spectra to observe the phosphorescence of SeP, if any. It is known that heavy atom substituents tend to reduce the fluorescence quantum yield ϕ_f in favor of phosphorescence emission ϕ_p causing $\phi_p/\phi_f > 1$. As ACN does not form glass at 77 K, the low temperature spectra were recorded using another polar solvent ethanol (EtOH) as rigid glassy matrix. Unfortunately in this matrix SeP does not emit phosphorescence. Thus the internal heavy atom effect on phosphorescence spectra of SeP was not clear. However in MCH rigid glassy matrix at 77 K SeP exhibits only fluorescence but no phosphorescence. Thus the low temperature event in this matrix differs from that observed at the ambient temperature where no detectable fluorescence was apparent. It seems as excitation was made in ^1L_a band (~ 330 nm), nonradiative relaxation required to come down to the lowest state $^1(n_O\pi^*)$, may not occur within the lifetime of the ^1L_a state at 77 K. This phenomenon is not rare at such low temperature as relaxation time increases due to lowering down of temperature. It seems logical to presume that fluorescence emission might mainly originate from ^1L_a level. However, to corroborate this proposition about the nature of the fluorescence emission band observed in MCH matrix at 77 K the steady state polarization measurements were done on the fluorescence excitation spectra of SeP which looks identical with its electronic absorption spectra. To record the excitation spectra the monitoring fluorescence emission wavelength was chosen at 400 nm position. Fig. 4 reproduces the polarized fluorescence excitation spectra of SeP in MCH rigid glassy matrix within the region of 320–380 nm which covers the envelop of ^1L_a band system.

It has been proposed above that the nature of 330 nm band observed in the electronic absorption spectra of SeP is mainly of character ^1L_a and ^1L_b band is hidden, as it was observed in cases of most acenes, within this ^1L_a envelop.

Fig. 4 shows depolarization effect both at the red edge and at the blue edge of the ^1L_a absorption band. Nearly at the middle of the band (around 345–355 nm region) positive values of degree of polarization, *P*, of moderate magnitudes were observed. As it is apparent from Fig. 2a at the blue edge of the 330 nm band there is a mixture of two states ^1B_b and ^1L_a. So this might cause depolarization. Moreover it is logical to presume that ^1L_b band might reside at the red edge of the ^1L_a band (generally ^1L_b possesses lower energetic level than ^1L_a). Thus at this edge also there might be a mixture of the two states ^1L_b and ^1L_a and this might cause depolarization in this region. In the middle of the ^1L_a band, which seems to be free from overlapping of ^1B_b or ^1L_b band system, positive degree of polarization value of moderate magnitude was observed. Thus it seems the majority contribution for fluorescence emission originates from ^1L_a state because had the emission been originated from ^1L_b state, the value of P in the middle of the spectra, which seems to be entirely within ^1L_a domain, should show negative value. However low positive value of P ($\sim$ 0.09) in the middle region of the ^1L_a absorption band indicates that even in this region mixing, of course of lesser extent, might exist between the ^1L_a state and the neighboring state ^1L_b (or ^1B_b).

3.2.2. *Why no phosphorescence was observed both in MCH and EtOH rigid glassy matrices at 77 K*

Two possible mechanisms have been proposed for the lack of phosphorescence of SeP in both MCH and EtOH rigid glassy matrix at 77 K. It is possible, as it was found in cases of some heterocyclic molecular systems [8], that the triplet levels corresponding to closely lying $^1L_b(\pi\pi^*)$ and $^1(n_O\pi^*)$ states are very close to each other as depicted in the Fig. 3. As these two triplet states are of opposite nature, $n\pi^*$ and $\pi\pi^*$, large vibronic interactions might occur within themselves and this might reduce the radiative transition probability from the lowest triplet state and simultaneously enhance the nonradiative transitions from this level.

As an alternative mechanism it could be suggested that in SeP due to presence of heavy atom Se nonradiative transition may be promoted largely through internal conversion (IC) process (^1L_a to S_0) rather than intersystem crossing. In favor of this argument it can be stated that in case of xanthene dyes it was observed [9] that with increase of the size of the halosubstituents (from chlorine to bromine to iodine) the phosphorescence lifetime decreases simultaneously with the quantum yield of the fluorescence and thus phosphorescence efficiency is not increased proportionally.

Next, we will discuss the possible role of SeP in bimolecular quenching reactions.

3.3. *Bimolecular photoprocesses*

Before going to study the bimolecular photoprocesses in which one of the reacting species is SeP, it seems important to measure its half-wave potential by electrochemical measurements to examine its electron donating or accepting ability.

3.3.1. *Electrochemical measurements*

From Table 1 it is seen that in ACN solvent SeP has a low positive value (0.7 eV) for half-

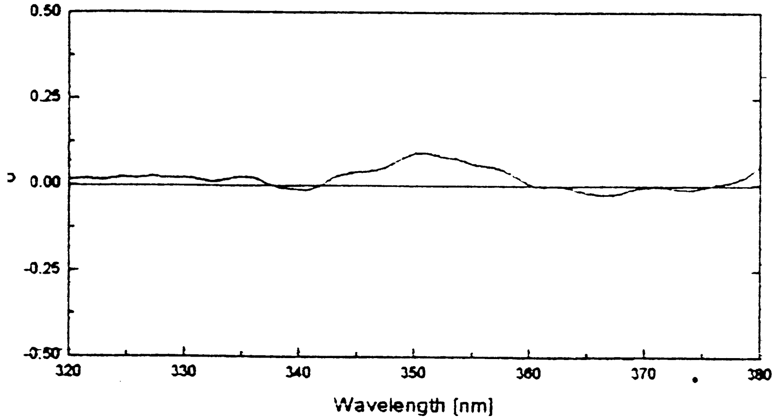

Fig. 4. Polarized fluorescence excitation spectra of SeP in MCH rigid glassy matrix ($\lambda_{em} \sim 400$ nm).

Table 1
Redox potential values, values of $E^*_{0,0}$ and Gibbs free energies (ΔG^0) for photoinduced electron transfer (ET) reactions within the present donor and acceptor molecules in highly polar solvent ACN at the ambient temperature

Donors	Acceptors	$E^{\text{ox}}_{1/2}$ (D/D) (V)	$E^{\text{red}}_{1/2}$ (A^-/A) (V)	$E_{0,0}$* (eV)	ΔG^0 (eV)
SeP	9CNA	0.7	−1.13		1.83
SeP	9CNA*	0.7	−1.13	3.08	−1.25
SeP*	9CNA	0.7	−1.13	3.7	−1.87

* Denotes the excited singlet state S_1.

wave oxidation potential measured by cyclic voltammetry (details are given in the experimental section). This shows SeP might behave as a strong electron donor when it would be sensitized with a suitable acceptor. In the present investigation we chose the well known acceptor 9CNA whose redox potential was found to be −1.13 eV (Table 1). The Gibbs free energy change (ΔG^0) associated with the electron transfer (ET) reaction for the present D-A systems are computed by using the well-known Rehm–Weller relation (1) [10,11]

$$\Delta G^0 = E^{\text{OX}}_{1/2}(\text{D}/\text{D}^+) - E^{\text{RED}}_{1/2}(\text{A}^-/\text{A}) - E^*_{0,0} - \frac{e^2}{4\pi\varepsilon_0\varepsilon_S R}. \quad (1)$$

As the contribution of the last term (coulomb stabilization term) is negligible in ACN solvent (~0.06 eV) [10,12], ΔG^0 values were computed by ignoring this term.

From Table 1 it is evident that photoinduced ET reactions between the donor SeP and the electron acceptor 9CNA is highly exergonic ($\Delta G^0 < 0$), i.e. energetically favorable when one of the chromophores are excited. However positive value of ΔG^0, observed from the unexcited reactants, demonstrates the fact that the possibility of occurrences of ET reactions in the ground state within the present reacting systems is very slim.

For the direct evidence of the occurrences of ET reactions the transient absorption spectra of the acceptor 9CNA in presence of the electron donor SeP was measured at the different delay times between the exciting and analyzing pulses by laser flash photolysis techniques. The results are described below.

3.3.2. Transient absorption spectra

With the help of Nd:YAG laser system pulsed laser excitation was made at 355 nm wavelength. This was done to excite only the acceptor moiety from the mixture of the donor SeP and the acceptor 9CNA in ACN solvent. This excitation produces a transient species which absorbs at 440 nm along with a weak shoulder at around 508 nm region (Fig. 5). Following the observations made earlier [13,14] the band at 440 nm may be assigned to the triplet–triplet absorption band of monomeric 9CNA. With increase of delay times from 0.4 μs to 1.4 μs to 2.4 μs, 440 nm band diminishes very fast relative to the shoulder at 508 nm. This indicates that the two different species should be responsible for these two bands.

The earlier flash photolysis experiment on 9CNA in ACN solvent showed that free 9CNA^- anion absorbs at 525 nm [12]. Thus in the present investigation, the transient band observed at 508 nm might possibly be due to tight contact ion-pair ($\text{SeC}^+/9\text{CNA}^-$) from which the radical anion of the acceptor species is accessible with the help of the present experimental set up. The interionic distance is much less in such type of contact ion pair than that of solvent separated ion-pair complex, due to which the free radical anionic species absorb at much longer wavelength region than the ions in the former complex. The geminate recombination takes place more efficiently in the tight contact ion-pair than dissociation into free radical ions and this causes the production of the monomeric triplet state of the excited species. Possibly this is the reason why much larger transient triplet absorption band of monomeric 9CNA is observed relative to its anion (Fig. 5), which appears as a shoulder at around 508 nm position (in inset of Fig. 5 magnified spectrum of the 9CNA$^-$ anion is shown). The observations of transient absorption bands of ion-pair were in accord to our expectation as the large negative values of ΔG^0 for the SeP–9CNA* system was observed (Table 1) from the electrochemical measurements.

As photoinduced ET reactions are nonradiative transitions, one should expect the quenching phenomena in the steady state fluorescence emission spectrum of the acceptor 9CNA in presence of the electron donor SeP in ACN solvent.

The results obtained from the fluorescence quenching studies at the ambient temperature have been presented below.

3.4. Fluorescence quenching phenomena of the acceptor 9CNA in presence of the electron donor SeP in ACN fluid solution at the ambient temperature

As photoinduced ET reactions are generally facilitated in highly polar medium ACN, investigations on quenching reactions were made in this solvent.

To keep in conformity with the transient measurements by flash photolysis techniques, the acceptor 9CNA was excited to its lowest excited singlet state (~ 377 nm) in presence of the unexcited donor SeP. From Fig. 6a it is apparent that at 377 nm position, where the acceptor 9CNA

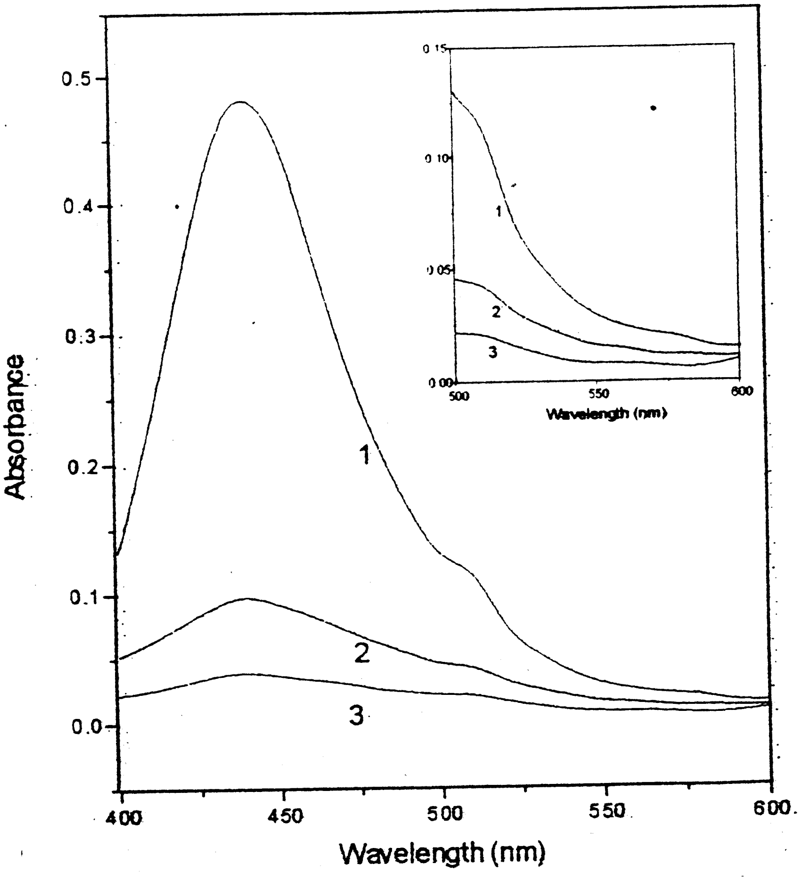

Fig. 5. Transient absorption spectra of 9CNA (excitation wavelength ~ 355 nm; third harmonic of Nd:YAG laser system), obtained by laser flash photolysis techniques, in ACN at the ambient temperature in presence of the donor SeP at the different delay times. The delay times are (1) 0.4 μs; (2) 1.4 μs; (3) 2.4 μs (inset shows the enlarged version of 500–600 nm wavelength range to demonstrate 9CNA$^-$ anionic band).

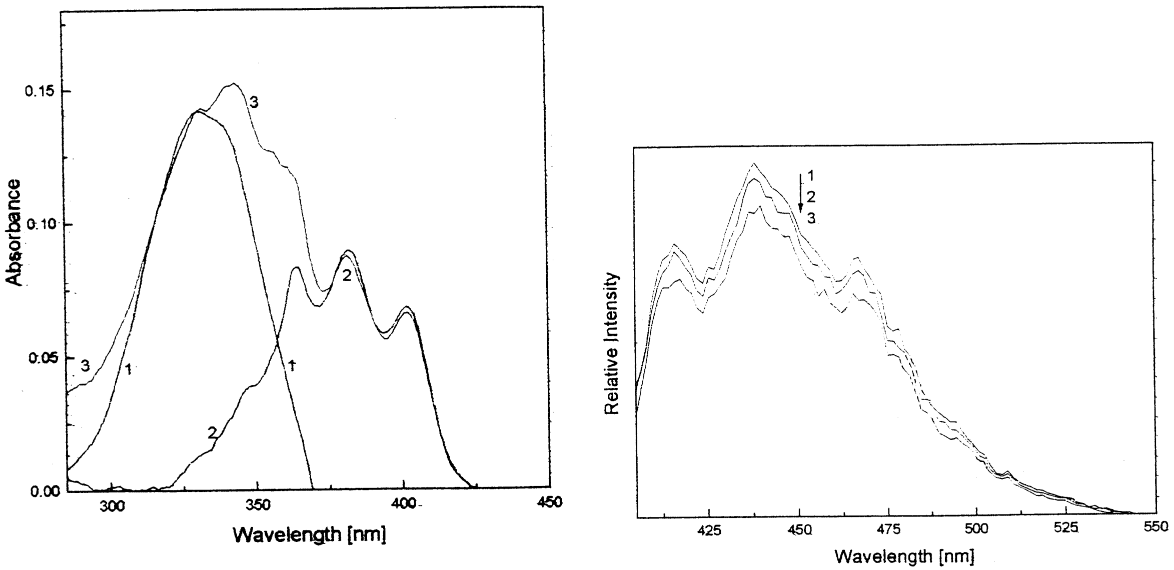

Fig. 6. (a) Electronic absorption spectra of the donor SeP (curve 1), acceptor 9 CNA (curve 2) and the mixture of the donor and acceptor (curve 3) in ACN solvent at the ambient temperature. (b) Fluorescence emission spectra of 9CNA fluorescer ($\lambda_{exc} = 402$ nm) in ACN solvent of concentration (2.78×10^{-6} mol dm^{-3}) at the ambient temperature in presence of the quencher (donor) SeP whose concentration (mol dm^{-3}) in (1) 0; (2) 2.00×10^{-5}; (3) 5.00×10^{-5}.

absorbs, the donor is completely transparent. Thus excitation at 377 nm avoids the competitive absorption by the donor as well as its filtering effect on the light emitted by the acceptor. From the same figure it is also found that the electronic absorption spectrum of the mixture of the donor and the acceptor in ACN is just the superposition of the individual absorption spectra of the interacting partners SeP and 9CNA. This observation excludes the possibility of the formation of ground state complex whose presence could be responsible for the observed fluorescence quenching of the acceptor 9CNA. Moreover, as the acceptor possesses lower lying electronic energy levels than those of the donor SeP, the energy transfer possibility, which is the another quenching reaction, is forbidden in the present case as the acceptor moiety was excited.

Thus the observed weak fluorescence quenching (Fig. 6b) might be due to photoinduced ET reactions whose existence within the present reacting systems has already been confirmed from the transient absorption measurements as discussed above. However, some sort of static quenching might also be operative. To test whether static component is present concurrently with the dynamic process ET in quenching mechanism, Stern–Volmer (SV) plot of fluorescence intensity variation of the acceptor (f_0/f) as a function of quencher (donor SeP) concentrations was drawn (D-A* system) [f_0 and f represent the relative integrated fluorescence emission intensities of the acceptor without and with the quencher (donor) concentration respectively]. As depicted in Fig. 7, SV plot shows clear positive deviation of quenching data from linearity and is found to be curved upwards. This phenomenon was observed in many cases of quenching studies where static quenching was present. However, unlike the situation generally observed in pure static quenching phenomena, the fluorescence lifetime of 9CNA was found to be affected significantly on gradual addition of the donor molecules SeP in ACN solvent (Table 2). This modifies our proposition made from SV plot and suggests that the quenching may not be pure static quenching in nature and the positive deviation from the simple SV relation might be introduced by the transient component of dynamic quenching. In favor of such proposition it could be mentioned that f_0/f

Table 2
Room temperature data on fluorescence lifetime (τ) of the acceptor 9CNA in presence of different quencher concentrations, values of K_{SV}, k_q, R, ΔG^0 and λ for 9CNA [a]–SeP system in ACN solvent

Conc. of 9CNA (mol dm^{-3})	Conc. of SeP (mol dm^{-3})	Solvent	τ ($\pm$0.4) (ns)	K_{SV} (dm^3 mol^{-1})	V (dm^3 mol^{-1}) (r/Å)	k_q (dm^3 mol^{-1} s^{-1})	R (Å)	ΔG^0 (eV)	λ (eV)
7.87×10^{-6}	0	ACN	11.5	0.07	13	6.4×10^6	10	-1.25	0.85
	6.95×10^{-7}		10.2		(17)				
	2.78×10^{-6}		9.1						
7.87×10^{-6}	0	EtOH	11.6	–	–	–	–	–	–
	1.11×10^{-5}		11.6						
	1.2×10^{-4}		11.7						

[a] Denotes the first excited singlet state. $\lambda(=\lambda_I+\lambda_s)$ was computed by using the procedure described elsewhere [10].

value, measured by steady state measurements, and value of τ_0/τ, measured by time resolved techniques, at the different donor (quencher) concentrations used are not similar to each other.

From the above observations it could be inferred that in overall quenching mechanism though dynamic quenching, through photoinduced ET process, is operative, the static (transient type) component is so overwhelming that the plot becomes curved upwards.

We computed Marcus first order ET rates k_{ET} for the present donor–acceptor system in ACN solvent by considering the relation (2) as used by earlier authors [15–18]

$$k_{\mathrm{ET}} = \frac{2\pi}{\hbar} \frac{J^2}{\sqrt{4\pi k_{\mathrm{B}} T \lambda_{\mathrm{S}}}} \exp\left[-\frac{(\Delta G^0 + \lambda_{\mathrm{S}})^2}{4 k_{\mathrm{B}} T \lambda_{\mathrm{S}}} \right] \tag{2}$$

$J^2 = J_0^2 \exp[-\beta(R - (r_{\mathrm{D}} + r_{\mathrm{A}})]$; J_0 denotes the transfer integral at $R = r_{\mathrm{D}} + r_{\mathrm{A}}$; β is the attenuation coefficient with R; the other symbols were described elsewhere [18].

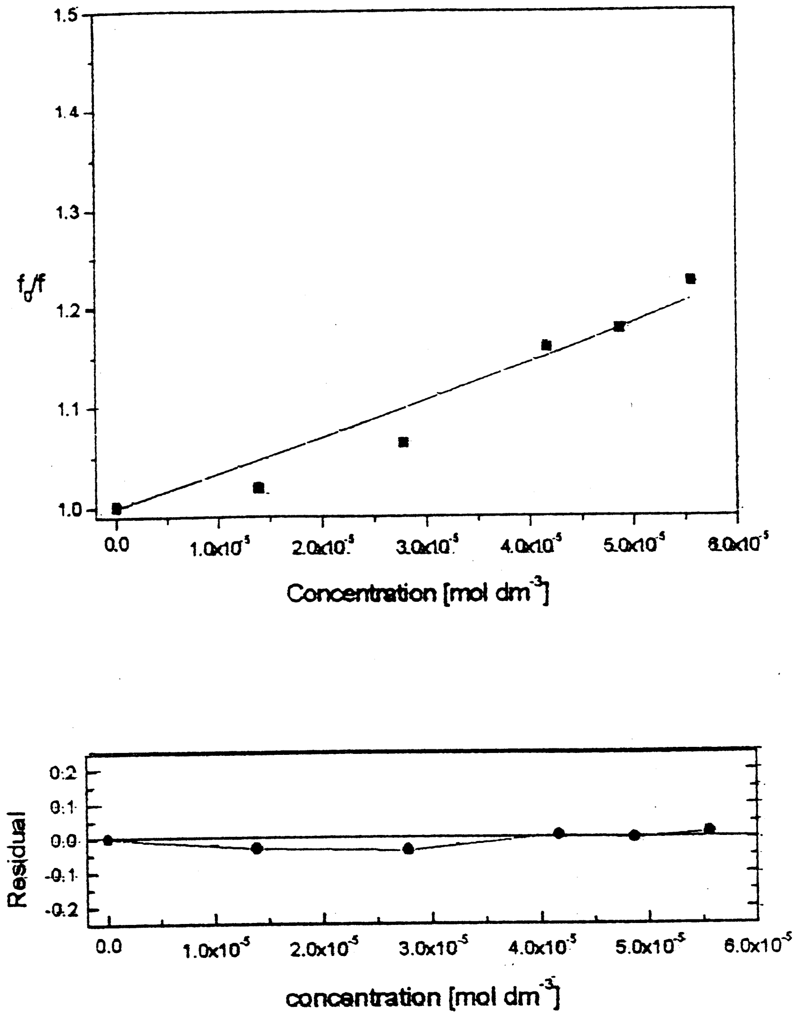

Fig. 7. Plot of f_0/f versus $[Q]$ of 9CNA*–SeP in ACN solvent at the ambient temperature. The nonlinear least square curve fitting procedure was used to treat the data according to the model: $f_0/f = (1 + V[Q])(1 + K_{\mathrm{SV}}[Q])(\exp k[Q])$ (see text), the graph of residual is plotted below.

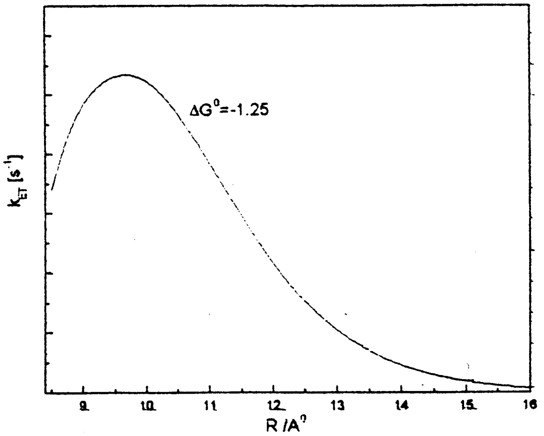

Fig. 8. Variation of first order electron transfer rate constant (k_{ET}) with the distance of separation (R/Å) between the present D and A molecules, where ΔG^0 is -1.25 eV. k_{ET} values were obtained theoretically by using Eq. (2).

Using the same procedure as adopted earlier [18], the dependence of k_{ET} on separation distance R is computed from the relation (2).

Fig. 8 represents the variation of k_{ET} with the distance of separation (R) between the present donor and acceptor systems. Clearly a maximum was observed in this curve as it could be expected for a highly exothermic reaction (ΔG^0 for SeP–9CNA* system in ACN ~ -1.25 eV). The maximum value of k_{ET} was found not at the encounter distance (~ 8.5 Å) but at somewhat higher distance (~ 10 Å, Fig. 8). It is logical to presume that at the separation distance $(R) \sim 10$ Å, the probability of occurrence of ET reactions should be maximum in ACN solvent.

From the above observations it seemingly indicates that in ACN environment a certain fraction of the excited states of 9CNA acceptor is actually quenched by ET mechanisms by the quenchers (SeP) which reside at a distance of 10 Å around the fluorophore 9CNA. But most of the excited states of the fluorophore are deactivated almost instantaneously just after being formed as a quencher molecule happens to be randomly positioned in the proximity (within the contact distance) of the fluorescer 9CNA at the time of excitation.

We tried to dissect the quenching data into its dynamic and static (instantaneous type) components by using the model used by Eftink and Ghiron (Eq. (3)) [19].

$$f_0/f = [1 + V(Q)](1 + K_{SV}[Q]) \tag{3}$$

where V is the transient (static type) parameter and K_{SV} is the collisional component. $1 + V[Q]$ is approximately equal to $\exp(V[Q])$. This assumptions was made by most of the authors to treat their data related to weak quenching reactions [19] which was actually observed in the present case.

The data were treated according to the above model (Eq. (3)), the modified form of SV relation, which comprises both static and dynamic part, but fitting seems to become much improved (normalization changes from 0.06 to 0.04) when an additional term $\exp(k[Q])$ is introduced as shown below:

$$f_0/f = (1 + V[Q])(1 + K_{SV}[Q])\ \exp(k[Q]) \tag{4}$$

It seems the quenching observed in the present case is somewhat complicated in nature and some other radiationless reactions, apart from ET and transient quenching, are also operative.

One possible reaction might be pure static quenching which possibly might interfere with the above two processes. Interestingly when the quenching measurements were done in another polar solvent EtOH, the same type of positive deviation in SV curve was noticed. But time resolved studies (by measuring fluorescence lifetimes) indicate that the nature of quenching here is slightly different from that observed in ACN. In EtOH, the fluorescence lifetime of the acceptor remains unaffected (Table 2) in the presence of the donor SeP. Thus the quenching might be assigned to pure static quenching unlike the situation observed in the case of quenching reaction between the same donor and acceptor system in polar aprotic ACN solvent where transient quenching (fluorescer lifetime changes in presence of the quencher molecule) seems to be operative as discussed above.

Thus it could be surmised that the mechanisms of bimolecular quenching processes involved within SeP and 9CNA systems seem to be the mixture of dynamic (photoinduced ET) and static type (both pure and transient) quenching modes, the existences of which are however, confirmed from both steady state and time resolved techniques. Further the possibility of external heavy atom effect on the fluorescence quenching of the acceptor 9CNA observed with gradual addition of the donor (quencher) SeP could not be ignored as the latter contains heavy atom 'Se'. Thus it can be inferred that in addition to the dynamic and static quenching, another quenching reaction 'external heavy atom effect' should possibly be involved in the overall quenching mechanism. Possibly due to presence of various quenching reactions, as proposed above, from the different experimental findings, the quenching data could not be fitted using the model proposed by Eftink and Ghiron which was used for the systems where only collisional (dynamic) and static modes were present. From the observations made in the present investigation, a model, as shown by Eq. (4), has been proposed where an additional parameter 'k' has been included in the proposed model of Eftink and Ghiron and the experimental quenching data fit in this model in a much better way as shown above. The best fit of the quenching data to Eq. (4) is reproduced in the Fig. 7.

The best fit values of K_{SV} and V are 0.07 and 13 $dm^3\ mol^{-1}$ respectively (Table 2). Large values (~ 3300) were observed in case of k which might arise from more than one quenching process (possibly from external heavy atom effect and static quenching).

The values of K_{SV} and V are in accord to our expectation. Very small value of K_{SV} (~ 0.07) indicate very weak dynamic quenching rate ($\sim 6.4 \times 10^6\ dm^3\ mol^{-1}\ s^{-1}$) which actually appears from the quenching studies as discussed above. From the value of $V(\sim 13\ dm^3\ mol^{-1})$, the radius r of the active volume was computed using the well-known relationship

$$\frac{V}{N'} = \frac{4}{3}\pi r^3$$ (N' is the Avogadro's number per mmol).

The value of r was estimated to be 17 Å. This indicates that at the exact moment of excitation the quencher may not be in physical contact with the fluorescer but it might happen that after the excitation of the 9CNA ring, the quencher (SeP) can diffuse the extra 8–9 Å (contact distance, $r_D + r_A \sim 8.5$ Å) so rapidly that the quenching still appears instantaneous. This points to the dynamic character predicted by the transient effect model [19]. Thus from the present investigation it may be surmised that SeP acts as a weak quencher but it shows diverse character in quenching mechanism of the excited singlet state (S_1) of the acceptor 9CNA. It deactivates nonradiatively the S_1 level of 9CNA as an electron donor as well as heavy atom quencher and also through pure static and transient quenching mechanisms.

From the present investigation it seemingly indicates that dynamic quenching is only due to presence of highly exothermic ($\Delta G^0 \sim -1.25$ eV) photoinduced ET process within the present reacting systems. The very weak, much smaller than the diffusion-controlled rate k_d in ACN ($\sim 1.9 \times 10^{10}\ dm^3\ mol^{-1}\ s^{-1}$) [20,21], dynamic quenching rate ($6.4 \times 10^6\ dm^3\ mol^{-1}\ s^{-1}$) points to the possibility of the occurrences of ET reaction in Marcus inverted region (mir) where outer sphere ET producing radical ion pair might not be so fast as to give diffusion controlled ET quenching rate. The possibility of occurrence of ET reaction in mir is further corroborated from the finding of larger $-\Delta G^0$ value than that of λ, nuclear reorganization energy parameter (Table 2). However for conclusive evidence for mir, investigations using other well known electron acceptors with SeP are needed. The work is under progress.

4. Concluding remarks

The newly synthesized selenophene compound SeP exhibits singlet ($n_0\pi^*$) in nonpolar MCH and $^1L_b(\pi,\pi^*)$ state in highly polar ACN as a lowest excited level. No emission was found from the former state, whereas a very weak fluorescence emission from the latter level possibly due to internal heavy atom effect was observed. The nonemissive behavior of the former state might be due to space forbiddenness with the ground side. The lack of phosphorescence of SeP has been inferred due to occurrence of vibronic interactions of the closely lying triplets $^3n_O\pi^*$ and $^3\pi\pi^*$. From the experimental findings and analysis of the quenching data it is revealed that primary contributions in fluorescence quenching of 9CNA in presence of SeP are due to static/instantaneous modes along with external heavy atom effect. Though the presence of highly exothermic photoinduced ET reactions within the present reacting system was confirmed from the measured values of ΔG^0 and transient absorption measurements using laser flash photolysis techniques, its role in overall quenching mechanism is not very significant as evidenced from observed upward curvature of SV plot. SeP seems to play diverse role in quenching mechanisms. Investigations with other electron acceptors are now underway.

Acknowledgements

We like to express our heartiest thanks to Dr Samita Basu of Saha Institute of Nuclear Physics, Calcutta for measurements of transient absorption spectra by laser flash photolysis techniques. S. K. De gratefully acknowledges the financial assistance from the UGC, New Delhi.

References

[1] D.E. Nixon, T.P. Moyer, M.F. Burrit, Spectrochim. Acta B 54 (1999) 931.
[2] B. Zelent, T. Ganguly, L. Farmer, D. Gravel, G. Durocher, J. Photochem. Photobiol. A: Chem. 56 (1991) 165.
[3] G.B.M. Bettolo, Gazz. Chim. Ital., 72, (1942), 201; Chem. Abs., 37, (1943), 4397.
[4] H.S. Mahal, H.S. Rai, K. Venkatarman, J. Chem. Soc., (1935), 866.
[5] K.B. Sharpless, K.M. Gordon, J. Am. Chem. Soc. 98 (1976) 300.
[6] E.J. Corey, J.P. Schaefer, J. Am. Chem. Soc. 82 (1960) 918.
[7] H.H. Jaffe, M. Orchim, Cations of Ultraviolet Spectroscopy, Wiley, New York, 1962, p. 345.
[8] S.K. Sarkar, T. Ganguly, Bull. Chem. Soc. Jpn. 63 (1990) 2372.
[9] K.K. Rohatgi-Mukherjee, Fundamentals of Photochemistry, Wiley Eastern, New Delhi, 1988, p. 144.
[10] T. Ganguly, D.K. Sharma, S. Gauthier, D. Gravel, G. Durocher, J. Phys. Chem. 96 (1992) 3757.
[11] S. Sinha, R. De, T. Ganguly, J. Photochem. Photobiol. A: Chem. 112 (1998) 13.
[12] B. Zelent, P. Messier, D. Gravel, S. Gauthier, G. Durocher, J. Photochem. Photobiol. A: Chem. 40 (1987) 145.
[13] E. Vander Dunckt, M.R. Barthels, A. Delestinne, J. Photochem. 1 (1973) 429.
[14] L.E. Manring, C. Gu, C.S. Foote, J. Phys. Chem. 87 (1983) 40.
[15] M. Maiti, S. Sinha, C. Deb, A. De, T. Ganguly, J. Luminescence 82 (1999) 259.
[16] S. Sinha, R. De, T. Ganguly, J. Phys. Chem. A 101 (1997) 2852.
[17] J.R. Bolton, J.A. Schmidt, T. Ho, J. Liu, K.J. Roach, A.C. Weedon, et al., in: J.R. Bolton, N. Mataga, G.L. Mclendon (Eds.), Advances in Chemistry Series 228, American Chemical Society, 1991, p. 117.
[18] A.K. De, T. Ganguly, Can. J. Chem. 78 (2000) 139.
[19] M.R. Eftink, C.A. Ghiron, J. Phys. Chem. 80 (1976) 486.
[20] P. Jana, R. De, T. Ganguly, J. Luminescence 59 (1994) 1.
[21] K. Kikuchi, J. Photochem. Photobiol. A: Chem. 65 (1992) 149.